EFFECT OF FLOW ON CALORIC CURVE FOR FINITE NUCLEI

S. K. Samaddar[1)], J. N. De[2)], and S. Shlomo[3)]

[1)] *Saha Institute of Nuclear Physics, 1/AF, Bidhannagar, Calcutta - 700064, India*

[2)] *Variable Energy Cyclotron Centre, 1/AF, Bidhannagar, Calcutta - 700064, India*

[3)] *Cyclotron Institute, Texas A&M University, College Station, TX 77843-3366, USA*

Abstract

In a finite temperature Thomas-Fermi theory, we construct caloric curves for finite nuclei enclosed in a freeze-out volume few times the normal nuclear volume, with and without inclusion of flow. Without flow, the caloric curve indicates a smooth liquid-gas phase transition whereas with flow, the transition may be very sharp. We discuss these results in the context of two recent experiments, one for heavy symmetric system (Au + Au at 600A MeV) and the other for highly asymmetric system (Au + C at 1A GeV) where different behaviours in the caloric curves are seen.

Keywords: Caloric curve; Specific heat; Collective flow; Thomas-Fermi; Phase transition

PACS numbers: 25.70.Pq,21.65.+f,24.10.Pa,25.75.Ld

Liquid-gas phase transition in nuclei is one of the fundamental issues driving intense studies in medium and high energy nuclear collisions in recent times. Theoretical studies on the equation of state (EOS) for infinite nuclear matter showed criticality at temperatures $T_c \sim 15 - 20$ MeV [1–3] depending on the interaction chosen and possible signals of such a critical behaviour were surmised from the power law distribution [4–7] of mass or charge fragments detected in energetic nuclear collisions. A clearer signal of liquid-gas phase transition in nuclei is hinted at from the experimental caloric curve [8] obtained in Au + Au collisions at 600A MeV where in the excitation energy range of $\sim$ 4-10 MeV per particle, the temperature T is found to be almost constant at a value of $T \sim 5$ MeV, even if there may be some uncertainty in the extraction of temperatures [9]. The specific heat at constant volume would then show a very sharp peak at this temperature and the excitation energy range over which T remains constant could be termed as the latent heat of vaporisation. On the theoretical side, fragmentation calculations in the microcanonical algorithm of Gross [10] and in the Copenhagen canonical description [11,12] show such a structure in the specific heat signalling a liquid-gas phase transition. The lattice-gas model for fragmentation [13] also shows such a peak. These trends in the caloric curve were seen in a very recent calculation [14] in the finite temperature Thomas-Fermi (FTTF) theory. Contrary to the extremely sharp peak at $T \sim 5$ MeV as inferred from the experimental caloric curve [8], the FTTF calculation showed a broad-based peak at $T \sim 9 - 10$ MeV depending on the system chosen.

Another set of experimental data with Au on C is reported recently [15] at a little higher energy (1A GeV) where the caloric curve is somewhat different; here around 6-7 MeV the temperature rises slowly but steadily with excitation energy, reminiscent of a continuous phase transition. These two different behaviours in the caloric curve reflect subtle changes in the physical process at different bombarding energies and for different systems and in the following, we try to explore and understand it within the framework of FTTF theory [16].

For a description of the hot nuclear material formed in energetic nuclear collisions, we consider a nucleus of N_0 neutrons and Z_0 protons, in thermodynamic equilibrium at a

temperature T within a 'freeze-out' volume V. In a generalised description, the systems may be initially compressed and because of decompression may have collective radial flow in addition to thermal excitation. An expanding system, in a strict thermodynamic sense, is not in equilibrium. However, if the time scale involved in the expansion is much larger compared to the equilibration times in the expanding complex, *i.e.* the flow velocity is quite small compared to the average nucleonic velocity, the assumption of thermodynamic equilibrium may not be inappropriate. In a recent paper, Pal et al [17] suggested to simulate the effect of collective radial flow through inclusion of an external negative pressure in the total thermodynamic potential at freeze-out volume. In absence of flow, at the freeze-out, the kinetic contribution of the thermal pressure is generally assumed to be cancelled by the interaction contribution, i.e, the system is at equilibrium under zero external pressure. A positive uniform external pressure gives rise to compression; similarly a negative external pressure gives rise to decompression resulting in the outward radial flow of matter. The expanding system can hence be assumed to be under the action of a negative external pressure P_0 , whose magnitude is equal to the flow pressure $P_f(|P_0| = P_f)$, the internal pressure exerted by the radially outgoing nucleons at the freeze-out surface. The total thermodynamic potential of the system [16] at freeze-out is given by

$$G = E - TS - \mu_n N_0 - \mu_p Z_0 + P_0\Omega, \tag{1}$$

where E and S are the energy and entropy of the system, respectively, μ_n and μ_p are the chemical potentials of neutrons and protons, respectively, P_0 the constant external pressure assumed negative and Ω the effective volume given by

$$\Omega = \frac{4}{3}\pi R_u^3, \quad R_u = (\frac{5}{3} < r^2 >)^{1/2}. \tag{2}$$

Here $< r^2 >^{1/2}$ is the root mean square radius (rms) of the matter density distribution and R_u is the radius of the corresponding uniform density distribution. We have taken this value of Ω in the present calculations. The interaction density is calculated with a Seyler-Blanchard type momentum and density dependent finite range two-body effective

interaction [16]; the Coulomb part with direct and exchange terms are included in this interaction density. Minimisation of the thermodynamic potential in the Thomas-Fermi approximation then leads to the expression for occupation probability as

$$n_\tau(r,p) = [1 + exp\{(\frac{p^2}{2m^*_\tau(r)} + V^0_\tau(r) + V^2_\tau(r) - \mu_\tau + P_0\frac{10\pi}{3A}R_u r^2)/T\}]^{-1}. \quad (3)$$

Here τ refers to neutrons or protons, V^0_τ is the single particle potential (which includes the Coulomb term for protons), m^*_τ the effective mass and V^2_τ the rearrangement potential that appears for a density dependent interaction. The density at any point is obtained from the momentum integration of the occupancy. The total energy density at temperature T is then written as

$$\varepsilon(r) = \sum_\tau \rho_\tau(r)[T\, J_{3/2}(\eta_\tau(r))/J_{1/2}(\eta_\tau(r))(1 - m^*_\tau(r)V^1_\tau(r)) + \frac{1}{2}V^0_\tau(r)]. \quad (4)$$

In Eq. (4), $J's$ are the usual Fermi integrals, V^1_τ is the potential term that comes with momentum dependence and is associated with m^*_τ. The fugacity $\eta_\tau(r)$ is defined as

$$\eta_\tau(r) = [\mu_\tau - V^0_\tau(r) - V^2_\tau(r) - P_0\frac{10\pi}{3A}R_u r^2]/T. \quad (5)$$

Once the interaction energy density is known, the nuclear density can be obtained self-consistently. The total energy per particle is then given by

$$e(T) = \int \varepsilon(r)\, d\mathbf{r}/A. \quad (6)$$

For details on the FTTF theory, we refer to Ref. [16].

For a finite system at nonzero temperature, the continuum states are occupied with a finite probability as a result of which the particle density does not vanish at large distances. The observables then depend on the size of the box in which the calculations are done. Guided by the practice that many calculations for nuclear collisions are done by imposing that thermalisation occurs in a freeze-out volume, we fix a volume and then calculate the caloric curve and thus the specific heat at constant volume.

In the present calculation, we choose the system ^{150}Sm which lies in the mass range of interest for the two experiments mentioned earlier. The freeze-out volume has been taken

to be $V = 8V_0$ where V_0 is the normal volume of the nucleus at zero temperature. This volume is close to the value generally used in statistical multifragmentation models [10,12] and to the one extracted from the double ratio of the isotope yields with inclusion of radial flow [18]. The physical observables of interest like phase transition temperature is found to be very weakly dependent on the freeze-out volume beyond $V = 8V_0$ as noted earlier [14]. In Figure 1, we display the caloric curve for ^{150}Sm. The excitation energy per particle e^* is defined as

$$e^* = e(T) - e(T = 0).$$

The caloric curves are shown for three values of pressures, namely, $P_0 = 0, -0.05$ and -0.1 MeV fm^{-3}. The flow pressure$P_f(= -P_0)$ is shown [17] to be related to the flow energy as

$$P_f = D(v_f, T)\rho(r)e_f(r), \tag{7}$$

where the quantity $D(v_f, T)$ depends weakly on the temperature T and the radially directed flow velocity v_f and is $\simeq 4.5$ for neutrons or protons [17] and $e_f(r)$ the flow energy per nucleon at any point within the volume. The total flow energy may be expressed as

$$E_f = \int_V \rho(r)e_f(r)d\mathbf{r} = P_f V/D(v_f, T). \tag{8}$$

The average flow energy per nucleon is then $\simeq 1.3$ MeV for $P_0 = -0.1$ MeV fm^{-3}. When there is no flow ($P_0 = 0$), the caloric curve is smooth with initial faster rise of temperature with excitation energy, then a slower rise and lastly a kink at $T \simeq 10$ MeV, after which the excitation energy rises linearly with temperature. With increase in flow energy, the rise in temperature is slower and when the pressure $P_0 = -0.1$ MeV fm^{-3}, the caloric curve shows a plateau at $T \simeq 5$ MeV in the excitation energy range of 5-10 MeV. In the above calculations, we have taken constant pressure independent of excitation energy. One expects however increase in flow energy with increasing excitation, which may influence a change in the caloric curve. To investigate this aspect, we take the flow energy and hence the external pressure proportional to T^2 as the excitation energy is not apriori known. Guided by the experimental data [8] that the slope of the linearly rising portion of the caloric curve is 3/2,

we further assume that the flow energy saturates at $T \simeq 5$ MeV. A representative calculation with the variable flow energy is also displayed in Figure 1 where the flow pressure saturates at a value P_0 = -0.1 MeV fm^{-3} at T=5.0 MeV. We find that the change in the caloric curve compared to that for constant pressure of P_0 = -0.1 MeV fm^{-3} is not significant. In Figure 2, the corresponding specific heat defined as

$$C_v = (de^*/dT)_v, \tag{9}$$

are displayed. The broad-based peak for no flow goes over to an extremely sharp peak from $T \simeq 9.5$ MeV to $T \simeq 5$ MeV with increasing flow. The structure of C_v and the other observables discussed subsequently for the variable flow reaching a saturation as mentioned are practically the same as those for constant pressure with the saturation value and therefore are not displayed in our results. Looking at Figures 1 and 2, it appears that the system signals a liquid-gas phase transition at the peak temperatures and with increase in flow energy, the system moves from a continuous phase transition to a sharp first order phase transition. The linear rise of excitation energy with temperature beyond the phase transition temperatures for all the cases in Figure 1 reflects the fact that the system behaves like a noninteracting gas of classical particles; the value of the slope there is 3/2, the classical value for C_v.

In Figure 3, the rms radius of the proton distribution for the system is shown as a function of temperature. For all the three cases with constant pressure, the radius initially increases very slowly with temperature and then the rise is very fast up to the phase transition temperature. For the cases accompanied with flow energy, there is an extremely sharp transition in the density distribution at the phase transition temperature as is evident from the very sharp increase in the rms radius. We have earlier noted [14] that when there is no flow, near the transition temperature within an interval of $\Delta T \sim 0.5$ MeV, the density distribution loses its structure and looks like a uniform distribution of matter inside the volume. With inclusion of flow energy, within an interval of $\Delta T \sim 0.1$ MeV near the transition temperature, the density distribution now undergoes an exotic shape transition

to a bubble shape at $T = 5.3$ MeV for $P_0 = -0.1$ MeV fm^{-3} which is displayed in Figure 4. The appearance of bubble-type configurations has also been noted earlier [19,20] in the dynamics of the expanding nuclei. A possible connection of these exotic shapes to first-order liquid-gas phase transition may be made from Figures 1 and 4. The slow fall in rms radius beyond the transition temperature (for non-zero flow) is found to be due to the filling up of the interior of the bubble.

We now make a comparison with the experimental data mentioned earlier. Both experiments refer to projectile fragmentation studies from far-central collisions, have little flow energy $\approx 0 - 2$ MeV per nucleon [21,22] and have a range of fragment masses studied from A ≈ 40 to A ≈ 200. We have therefore repeated the calculations for a spectrum of masses in the mass range of experimental interest. We find [23] nearly the same behaviour in the caloric curve with transition temperatures differing at most by ≈ 0.2 MeV in the case with $P_0 = -0.1$ MeV fm^{-3}. The Au+Au data at 600 A.MeV fit extremely well with the theoretical results with $P_0 = -0.1$ MeV fm^{-3} which corresponds to a flow energy of ≈ 1.3 MeV per nucleon. The Au+C data at the higher energy of 1 A.GeV also fall in the band of theoretical results calculated with P_0 between 0.0 to -0.1 MeV fm^{-3}. Here the target is very light and a lesser compression or lower flow energy is expected. We calculated the incompressibility of the nuclei in the scaling model as a function of temperature and found that in both cases with or without flow, the incompressibility vanishes at the transition temperature which may add further as a positive signal to liquid-gas phase transition [23].

To summarise, we have calculated the caloric curve and the specific heat of a finite nucleus with mass in the range of experimental interest in a self-consistent finite temperature Thomas-Fermi theory with and without any collective radial flow and find signals of liquid-gas phase transition in both cases. In the case without flow, there appears to be a continuous phase transition at a temperature $T \simeq 9.5$ MeV, much below the critical temperature for infinite nuclear matter ($T_c \simeq 16$ MeV) whereas with inclusion of a nominal flow energy of ~ 1.3 MeV per nucleon, the transition appears to be a first order phase transition at $T \simeq 5$ MeV. In the latter case, there is in addition a phase transition to a bubble shape from

a diffuse spherical shape. The conclusions remain unaltered even if an excitation energy dependent flow as mentioned earlier is employed. The bubble shape may be an artifact of the spherical symmetry imposed in the FTTF calculation; if such constraints were relaxed, different shapes like a torus might have been obtained. The problem, however, then becomes numerically more involved. The theoretical results fit extremely well with the experimental data. In the higher energy 1 A GeV Au on the very light C nucleus, the projectile-like fragment suffers possibly very little or no compression and then the caloric curve alludes to a continuous phase transition. For the lower energy 600 A MeV Au+Au, slight compression leading to a modest radial flow energy may not possibly be ignored and then changes in the caloric curve may result as is indicated in the experiments.

The authors express their sincere thanks to Prof. S. Dasgupta discussions with whom initiated this work. This work is partially supported by the U.S. National Science Foundation under grant No. PHY-9413872.

REFERENCES

[1] W. A. Kupper, G. Wegmann and E. R. Hilf, Ann. of Phys., **88**, 454 (1974).

[2] H. Jaqaman, A. Z. Mekjian and L. Zamick, Phys. Rev. C**27**, 2782 (1983); **29**, 2067 (1984).

[3] D. Bandyopadhyay, C. Samanta, S. K. Samaddar and J. N. De, Nucl. Phys. **A511**, 1 (1990).

[4] J. E. Finn et al., Phys. Rev. Lett.. **49**, 1321 (1982).

[5] R. E. L. Green, R. G. Korteling and K. P. Jackson, Phys. Rev. C**29**, 1806 (1984).

[6] C. B. Chitwood, D. J. Fields, C. K. Gelbke, W. G. Lynch, A. D. Panagiotou, M. B. Tsang, H. Utsunomiya and W. A. Friedmann, Phys. Lett.. B**131**, 289 (1983).

[7] U. Lynen et al., Nucl. Phys. A**387**, 129c (1982).

[8] J. Pochodzalla et al., Phys. Rev. Lett.. **75**, 1040 (1995).

[9] X. Campi, H. Krivine and E. Plagnol, Phys. Lett.. B **385**, 1 (1996).

[10] D. H. E. Gross, Rep. Prog. Phys. **53**, 605 (1990).

[11] J. P. Bondorf, R. Donangelo, I. N. Mishustin and H. Schultz, Nucl. Phys. A**444**, 460 (1985).

[12] J. P. Bondorf, A. S. Botvina, A. S. Iljinov, I. N. Mishustin and K. Sneppen, Phys. Rep. **257**, 130 (1995).

[13] S. Das Gupta, J. Pan, I. Kvasnikova and C. Gale, to be submitted for publication.

[14] J. N. De, S. Dasgupta, S. Shlomo and S. K. Samaddar, Phys. Rev. C (April 1997, in press).

[15] J. A. Hauger et al., Phys. Rev. Lett. **77**, 235(1996).

[16] J. N. De, N. Rudra, Subrata Pal and S. K. Samaddar, Phys. Rev. C **53**, 780 (1996)

[17] Subrata Pal, S. K. Samaddar and J. N. De, Nucl. phys. A **608**, 49(1996).

[18] S. Shlomo, J. N. De and A. Kolomiets, Phys. Rev. C (May 1997, in press).

[19] C. Y. Wong, J. A. Maruhn and T. A. Welton, Phys. Lett.. B **66**, 19 (1981).

[20] J. Nemeth, M. Barranco, C. Ngo and E. Tomasi, Z. Phys. A **323**, 419 (1986).

[21] U. Lynen, Talk in the Sixth International Conference on Nucleus-Nucleus collisions, Gatlinburg, June 2-6 (1997).

[22] D. Durand, *ibid.*

[23] J. N. De, S. K. samaddar and S. Shlomo (to be published).

FIGURE CAPTIONS

Fig. 1 The excitation energy per particle plotted as a function of temperature (caloric curve) for the system ^{150}Sm at freeze-out volume $V = 8V_0$. The dotted, dashed and the full lines correspond to $P_0 = 0.0, -0.05$ and -0.1 MeV fm^{-3}, respectively. The dash-dotted line corresponds to variable pressure (see text). The data are taken from Ref. [8] (full squares) and from Ref. [15] (open circles).

Fig. 2 The specific heat per particle plotted as a function of temperature for the system ^{150}Sm with $V = 8V_0$. The dotted, dashed and the full lines have the same meaning as in Fig. 1.

Fig. 3 The proton rms radius is plotted as a function of temperature for the system ^{150}Sm. The symbols have the same meaning as in Fig. 1.

Fig. 4 The proton density profile for the system ^{150}Sm calculated with $P_0 = -0.1$ MeV fm^{-3} and $V = 8V_0$. The dashed and the full lines correspond to T= 5.2 and 5.3 MeV, respectively.

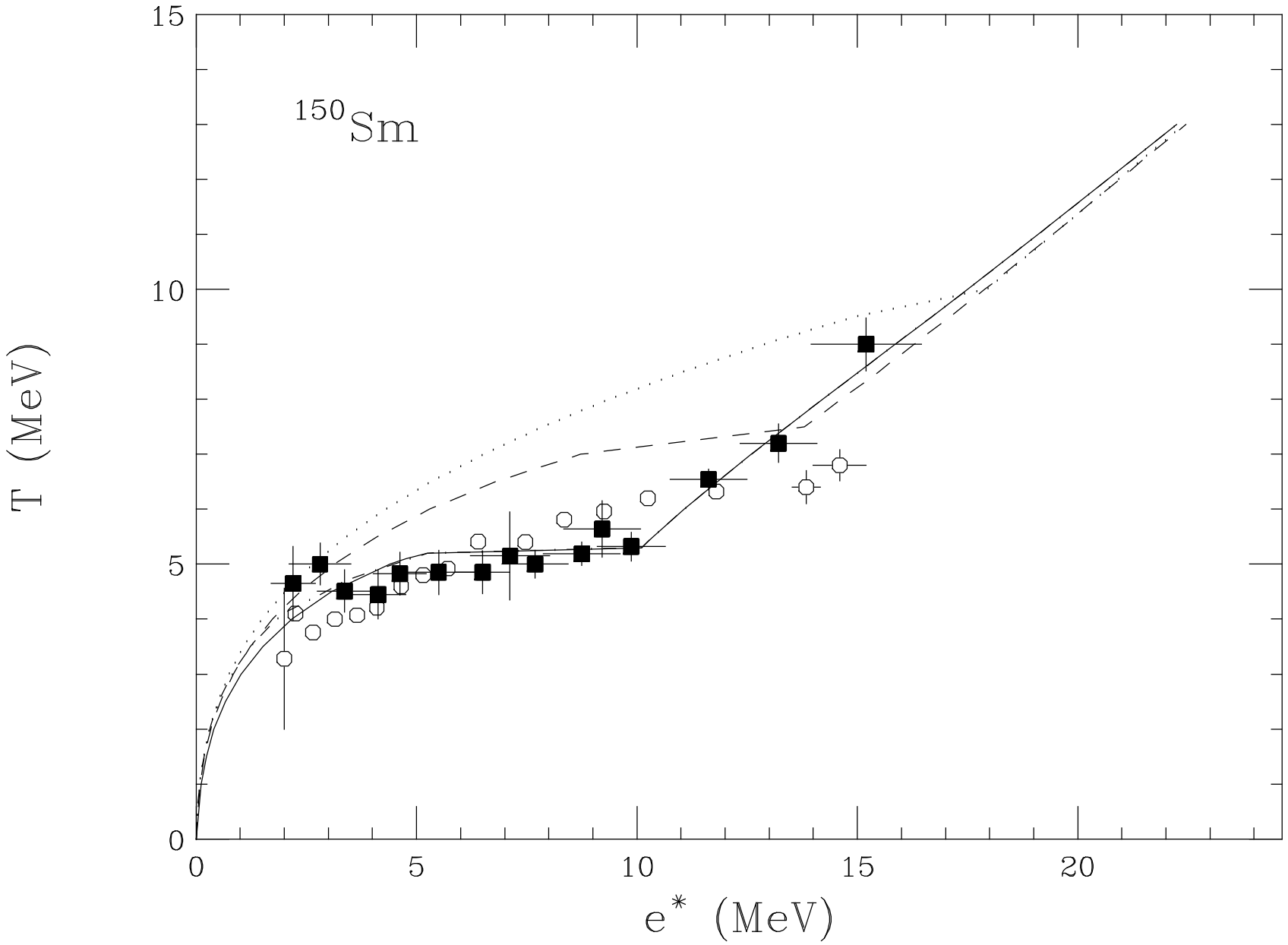
^{150}Sm
T (MeV)
e* (MeV)
0
5
10
15
20

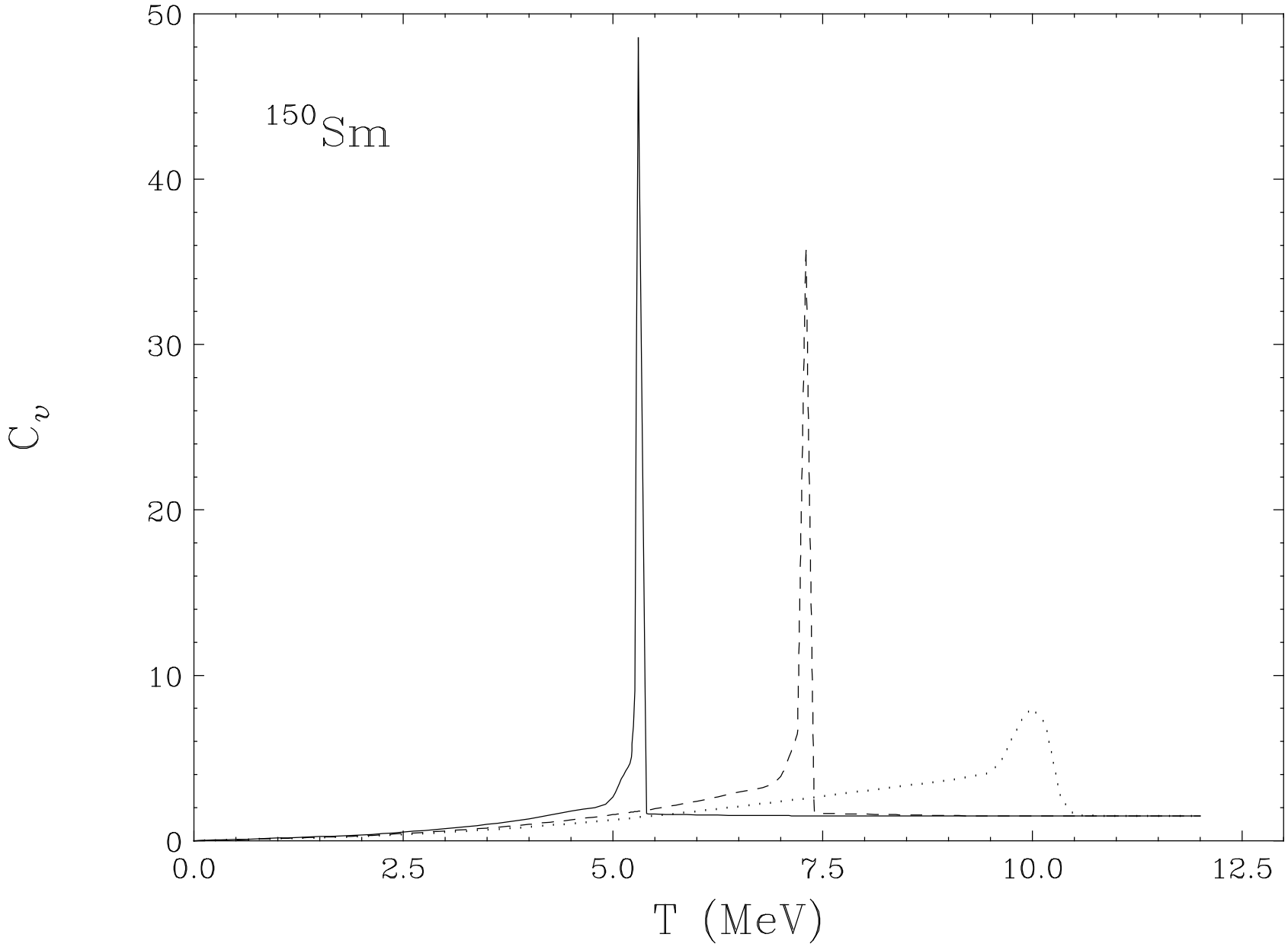
^{150}Sm
C_v
T (MeV)
0
10
20
30
40
50
0.0
2.5
5.0
7.5
10.0
12.5

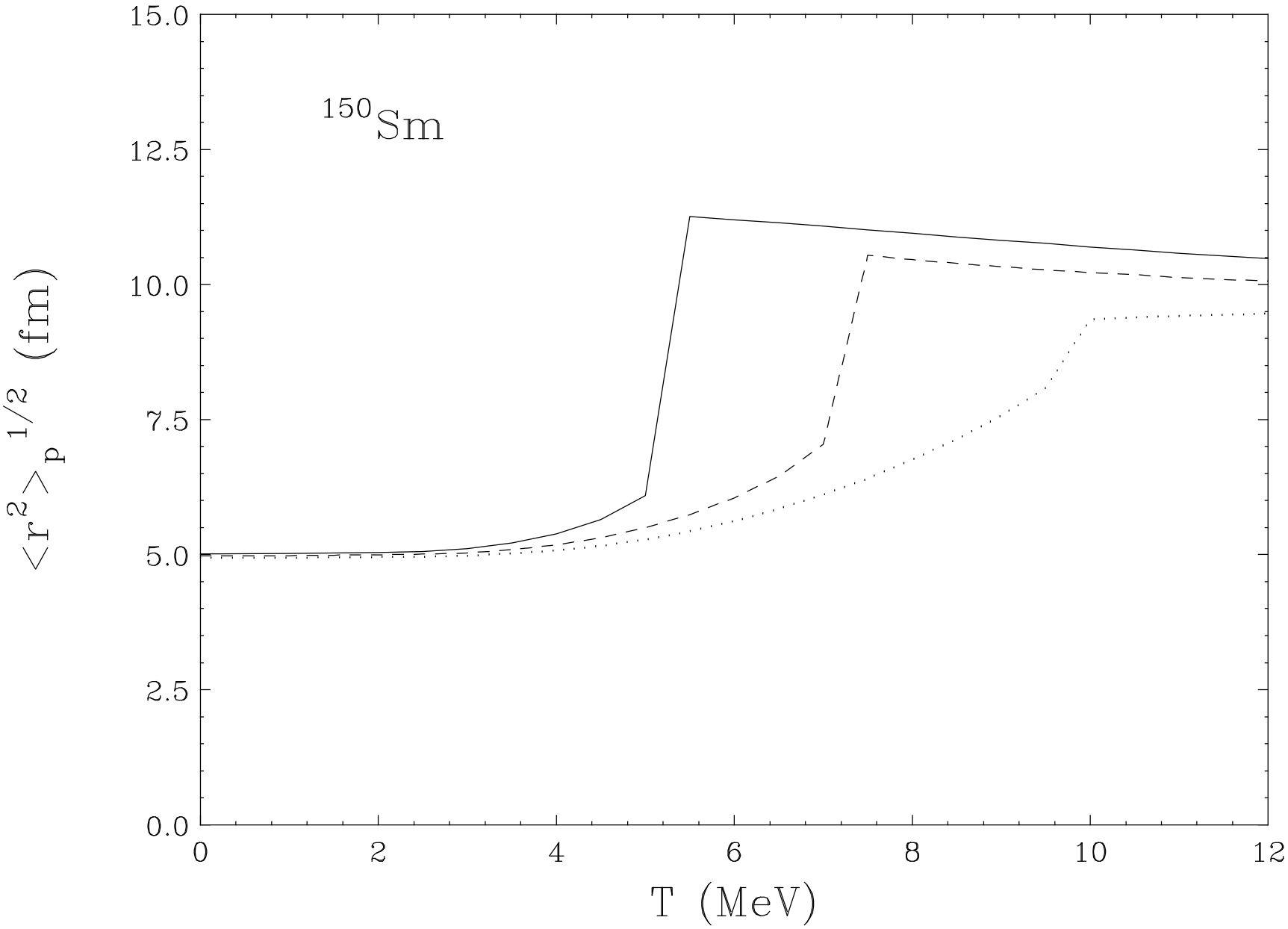
^{150}Sm
$\langle r^2 \rangle_p^{1/2}$ (fm)
T (MeV)
0.0
2.5
5.0
7.5
10.0
12.5
15.0
0
2
4
6
8
10
12

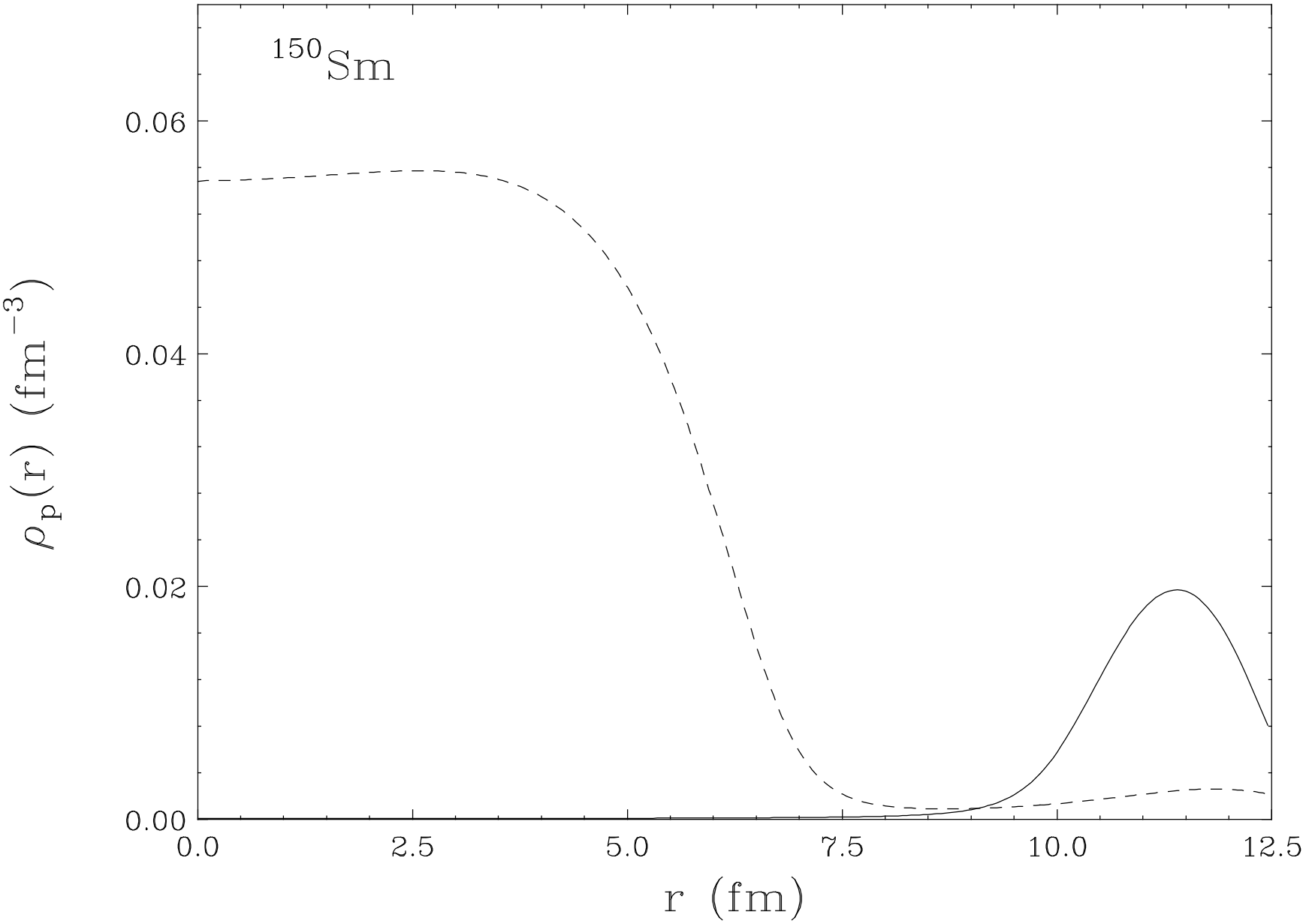
^{150}Sm
0.06
0.04
0.02
0.00
$\rho_p(r)$ (fm^{-3})
0.0
2.5
5.0
7.5
10.0
12.5
r (fm)